Absolute rate parameters for infrared photochemistry: $CF_3I \rightarrow CF_3 + I$

M. Quack and G. Seyfang

Insitut für Physikalische Chemie der Universität, Tammannstraße 6, D-3400 Göttingen, West Germany

(Received 23 July 1981; accepted 29 September 1981)

IR-photolysis yields are reported for CF_3I irradiated with the R14 line of the $(001 \rightarrow 02^00)$ transition of a pulsed TEA-CO_2 laser (at 1074.65 cm^{-1}) with unstable resonator optics providing a smooth and well-defined fluence profile in the far field. The reaction products ($CF_3 + I$) of the primary reaction are scavenged by reactions with added NO, Br_2, or ClNO in order to reliably establish the primary yields. A data treatment valid for arbitrary, smooth spatial fluence profiles is proposed for the evaluation of true yields and rate coefficients $k_I(st)$. The influence of collisions with buffer gas molecules on the evaluation of $k_I(st)$ is investigated in experiments and by model calculations. A steady state rate coefficient for the unimolecular decomposition of CF_3I under irradiation with constant intensity I is obtained to be $k(st) = 10^{(6.2 \pm 0.3)}$ $(I/\mathrm{MW\ cm^{-2}})\mathrm{s}^{-1}$ valid for intensities near and above 100 MW cm^{-2}. This is consistent with a low *a priori* estimate of rate coefficients from a simple theoretical model involving only easily measurable molecular properties. The physical significance of this absolute rate parameter is discussed.

I. INTRODUCTION

Unimolecular reactions induced by monochromatic infrared radiation (URIMIR) constitute a rapidly developing, new area of research in chemical kinetics and photochemistry.[1-3] Many experiments have so far dealt with qualitative, mechanistic aspects of these reactions and the underlying multiphoton excitation processes. Less attention has been paid to the definition and experimental determination of suitable kinetic parameters characterizing these reactions quantitatively. The primary data in IR photochemistry can be expressed through the reactant concentration c_R remaining after irradiation with a certain radiation frequency of intensity I, during a time t or with a fluence F

$$F(t) = \int_0^t I(t')\,dt' \ , \tag{1}$$

$$c_R/c_R^0 = F_R = 1 - F_P = f(F, I, t) \ . \tag{2}$$

For irradiation with uniform intensity Eq. (2) may be considered to contain two degrees of freedom (for the three independent variables F, I, and t), but in general there is arbitrary complexity contained in the function $I(t)$. From the reactant concentration one can derive the time dependent rate coefficient

$$k(F, I, t) = -\frac{d \ln F_R}{dt} \ . \tag{3}$$

As in ordinary kinetics the rate coefficient might be measured by following the reactant concentration as a function of time during irradiation pulses with constant and well defined intensity. Such well defined irradiation conditions have been achieved only recently[4] and in practice a simpler approach may be useful.

Under certain conditions[5,6] (irreducible rate coefficient matrix), k approaches its constant steady state value $k(st)$, typically after about 20%–30% reaction ($F_R < 0.8$), within a factor of 2. $k(st)$ depends only upon the radiation intensity (and frequency) and molecular properties. It corresponds in many respects to the rate constant in ordinary chemical reactions. It has been shown[7] that $k(st)$ can be derived, in principle, from experiments measuring the total yield $F_P^* = 1 - F_R^* > F_P$ (including reaction after the end of irradiation) from the limiting slope in the logarithmic reactant fluence plot

$$\lim\left(-\frac{d \ln F_R}{dF}\right) = k(st)/I = k_I(st) \ . \tag{4}$$

$k_I(st)$ is a weak function of intensity in the linear regime of IR photochemistry (case B of Ref. 5). We think that it provides the best way to characterize, for a given molecule, the rate by a single parameter over moderate ranges of intensity [of course, more than one parameter is needed for the full dependence in Eq. (3), see below] It is the purpose of the present paper to discuss with a specific experimental investigation, which precautions have to be taken in practice, in order to obtain absolute, reliable values of $k_I(st)$, which are transferable from one laboratory to another (independent of special laser properties). When such quantitative, unique rate parameters are established, one may ask in a meaningful way, how they depend upon molecular properties.[8] This question will be dealt with in reports on further experiments.[9]

The model reaction chosen here is

$$CF_3I + nh\nu \rightarrow CF_3 + I \ . \tag{5}$$

The first report on multiphoton excitation of CF_3I dates back to 1976.[10] Reaction yield data were obtained in an investigation of carbon isotope separation by Bittenson and Houston.[11] These data were used for one of the first illustrations of the general method for determining $k(st)$.[7,12] Beam data have established the primary Reaction (5) beyond doubt[13] and a number of further experimental studies of the multiphoton excitation and dissociation of CF_3I have appeared.[14-18] The IR spectroscopy of CF_3I and the thermochemistry of Reaction (5) are fairly well established.[19] Furthermore, the URIMIR of CF_3I has been the subject of several model calculations.[6,8,20-22] Rate coefficients for CF_3I and some other molecules have been evaluated from semiquantitative data from the literature, which had not been obtained in view of absolute $k(st)$, and have been summarized in.[23] These investigations and the fact that CF_3I is expected

0021-9606/82/020955-11$02.10

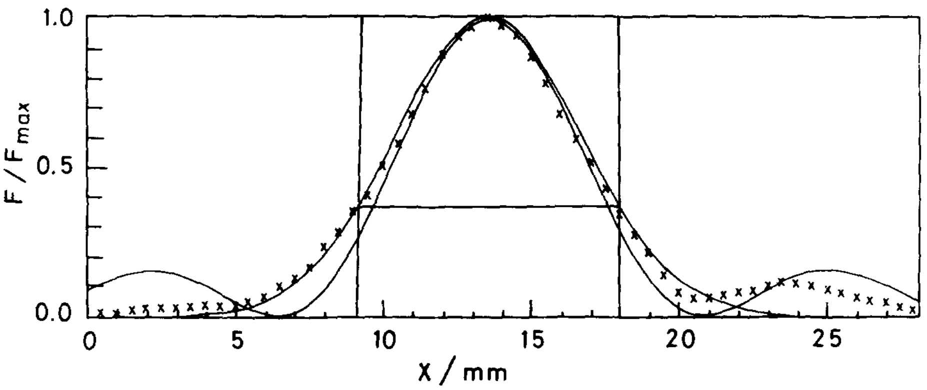

FIG. 1. Fluence profile measured across the beam in the far field (30 m) of the CO_2-TEA laser with unstable resonator optics (crosses). The full lines indicate Gaussian and Bessel-type theoretical functions. The rectangle indicates a nominal fluence profile with a nominal beam diameter. (See also the Discussion in the text.)

to have a very high $k_I(st)$ provide a good starting point. On the other hand, in quantitative terms the previous work leaves some room for improvements as will be seen from the new results reported here. We shall present appropriate techniques for the quantitative evaluation of bulk yield data in terms of $k(st)$. The effect of uncontrolled or difficult to control laboratory variables and the effect of inert gas pressure in the evaluation of $k(st)$ will be discussed.

II. EXPERIMENTAL

The source of the monochromatic IR radiation used is a TEA-CO_2-laser (Lumonics 103-2), grating tuned to individual lines, which were measured with a grating monochromator. The laser was fitted with unstable resonator optics providing essentially single transverse mode operation.[24,25] The far-field (25 to 35 m) of the laser was used for sample irradiation. The spatial characteristics of a typical fluence profile measured across the beam with a diaphragm of diameter $d < 2$ mm is shown in Fig. 1 (crosses: experiment, lines: theoretical functions, Gaussian or Bessel type, see Refs. 24 and 25). It is essential for the data treatment presented below, that the spatial fluence profile is known to be a smooth, accurately measurable (otherwise arbitrary) function. This is one reason for choosing unstable resonator optics, which, however, reduces somewhat the total output energy of the laser. In practice, the main peak is close to symmetric about the beam axis, whereas the wings show deviations from axial symmetry (see Refs. 24 and 25 for a detailed discussion, not directly relevant in the present context). The diameter of the beam and the value of F_{max} could be varied by placing the sample cells at different distances of mirrors with radius of curvature $r = 20$ m or $r = -10$ m, respectively, or by reducing the beam with a diaphragm in the near field, 20 cm behind the output mirror. The change of F_{max} over the lengths of the sample cells was always negligible. The total pulse energy was measured with pyroelectric detectors (Lumonics 50 D and 20 D), which were calibrated by comparison with several absolutely calibrated detectors of the pyroelectric and calorimetric type. The energy measurement is estimated to be accurate to 10%, the relative accuracy being much better. The laser was operated at frequencies of less than 0.5 Hz (in some control experiments less than 0.01 Hz).

The temporal intensity profile of one laser pulse measured with a photon drag detector (Rofin) and a 100 MHz oscilloscope (Tektronix, risetime 3 ns limiting factor in the time resolution) is shown in Fig. 2. It consists of several short, intense pulses due to longitudinal mode beating and partial self-mode-locking.[26,27] In contrast to the total pulse energy and the spatial fluence profile, the time dependent intensity is not exactly reproducible from shot to shot and therefore, not an accurately controlled experimental parameter, as is true for most experiments in this field, with the notable exception of Ref. 4, where intensity has been perfectly controlled. However, the high intensity spikes in Fig. 2 are favorable for URIMIR and the intensity control in the present example is less important for the evaluation of $k_I(st)$, as is discussed below. Operation with standard He/CO_2 mixtures of the lasing gas provides intensity profiles as shown in Fig. 2, referred to as short pulses hereafter. Adding N_2 to the gas mixture gives a similar shape but in addition a low intensity tail of about 1 μs length containing about one third of the pulse energy, referred to as long pulses hereafter.

Three sample cells fitted with KCl windows were used, two glass cells of optical path 10 and 20 cm, respective-

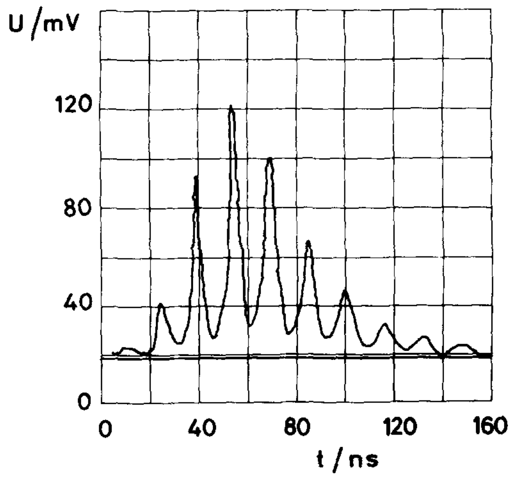

FIG. 2. Output voltage of a photon drag detector, measured with a 100 MHz oscilloscope for a CO_2-laser pulse (without tail). Subject to the limited time resolution the function is approximately proportional to the time dependent laser intensity (the baseline is the line just below 20 mV).

ly, and a stainless steel cell, optical path 10 cm. No significant variation in the yield P_{app} (see below) as a function of cell length, volume, and material was observed. For reaction yield measurements the CF_3I pressure was always chosen such (< 13 Pa) that the change of the laser fluence was less than 2% over the cell length and no measurable distortion of the spatial or temporal profile occurred. This is important for an accurate definition of the radiation properties in the cell volume. At high partial pressures of CF_3I ($\geqslant$ 130 Pa) significant absorptions and distortions are observed. Total pressures were measured with Setra capacitance manometers, absolutely calibrated with Hg manometers, with dibutylphtalate manometers and by expansion into known volume ratios. Partial pressures of reactants and products were measured by quantitative IR-spectroscopy with a Zeiss IMR25 spectrometer. All molecules discussed below can be separately measured by their strongest bands except the pair CF_3NO and C_2F_6, for which overlapping occurs. Relative product yields were also measured by gaschromatography (Siemens L 402), using a thermal conductivity detector and Porapack Q columns (T variable < 350 K, l = 2 m).

The primary reaction in the IR photolysis of CF_3I is given in Eq. (5).[11,13,14] It is followed by:

$$CF_3 + I(+M) \rightarrow CF_3I(+M) \ , \qquad (6)$$

$$2CF_3(+M) \rightarrow C_2F_6(+M) \ , \qquad (7)$$

$$I + I(+M) \rightarrow I_2(+M) \ . \qquad (8)$$

If I_2 is present (we have prevented this in some experiments by trapping the I_2 in a cold finger) one also has

$$CF_3 + I_2 \rightarrow CF_3I + I \ . \qquad (9)$$

The major reaction reducing the total yield below the primary photolysis yield is Reaction (6), which is of about the same rate as Reaction (7).[11] In order to prevent Reaction (6), the CF_3 radicals were scavenged by adding an excess of about 130 Pa of either NO, ClNO, or Br_2

$$CF_3 + NO(+M) \rightarrow CF_3NO(+M) \ , \qquad (10)$$

$$CF_3 + Br_2 \rightarrow CF_3Br + Br \ , \qquad (11)$$

$$CF_3 + ClNO \rightarrow CF_3Cl + NO \qquad (12)$$

$$\rightarrow CF_3NO + Cl \ . \qquad (13)$$

Reaction (13) is probably unimportant, as are several further possible reactions, e.g., $CF_3I + Br$, etc.

The presence of NO also catalyzes Reaction (8).[28] The rate coefficients for the recombination Reactions (6), (7), and (10) in the fall-off are not exactly known, but can be estimated theoretically.[30] The rates of the bimolecular Reactions (11) and (12) have been measured recently.[29] *By measuring all product yields one is thus* able to estimate all rate constants and obtain the primary yield. These fairly uncertain rate constant estimates are not given here, since in practice the conditions were chosen such that C_2F_6 formation (and therefore also $CF_3 + I$ recombination) was suppressed, except for some runs with pure CF_3I and the runs with small partial pressures of NO and high fluence (and therefore high $[CF_3]$ and $[I]$), for which there was some C_2F_6 product. No C_2F_6 product is observed with $p_{NO} > 2.5 \times 10^3$ Pa. The role of the collisions of the excited reactant with the scavenging gases on the determination of $k_I(st)$ is discussed in Sec. III. Reactive bimolecular collisions of the laser excited CF_3I with the radical scavengers can be excluded, because the same photolysis yield is obtained with all scavengers. In preliminary experiments we also used O_2 as scavenger[17] (giving CF_2O as final product), but this was abandoned because of the ill defined chemistry involved. HI has also been used for scavenging CF_3 in the IR photolysis of CF_3I.[11]

All measurements were carried out at room temperature. In order to test for any possible thermal contribution to the CF_3I decomposition, due to the temperature rise in the sample mixture after irradiation, we have measured the yields as a function of $[CF_3I]_0$ at fixed total pressure. This changes the absorbed energy ($\propto [CF_3I]_0$) and the temperature rise, which can also be calculated approximately. No thermal contribution to the decomposition of CF_3I under our conditions is observed. The yields reported below are thus firmly established to approximate closely the primary photolysis yields of Reaction (5). The fraction f of reactant decomposed per pulse in the photolysis cell is obtained from the measurements of reactant decay (and product formation) as a function of the number n of the laser pulses through Eq. (14)

$$[CF_3I]_n = [CF_3I]_0 (1 - f)^n \ . \qquad (14)$$

From f one can calculate the apparent product yield P_{app} in the irradiated volume V_I (V_c is the cell volume)

$$P_{app} = f(V_c/V_I) \ . \qquad (15)$$

V_I is *defined* by the effective beam diameter shown by the rectangle in Fig. 1, with the nominal (rectangular) fluence profile corresponding to F_{max} giving the correct overall pulse energy. It should be stressed that Eq. (15) in the present work is just a normalization without physical significance, the real yield and rate coefficient being obtained by the procedure discussed in Sec. III. Often, in IR photochemistry P_{app} has been identified with the real yield F_p^* at fluence F, which may be quite incorrect, since even $P_{app} > 1$ is possible (whereas $F_p^* > 1$ is clearly meaningless). The size of the errors introduced by setting approximately $P_{app} \simeq F_p^*$ depends upon the fluence profile, and is of no concern to us here. The chemicals were available commercially (CF_3I, PCR-Ventron, CF_3NO, NO, and ClNO, Matheson, Br_2, Merck Darmstadt). Their purity and identity was checked by gaschromatography and IR spectroscopy. They were purified by trap to trap distillation, when necessary (notably ClNO). All samples were then stored in direct connection to the vacuum line and thoroughly degassed by several freeze–thaw cycles before use.

III. RESULTS AND DISCUSSION

A. Method of data evaluation

The method of evaluation of the primary data in IR photochemistry used for extracting meaningful quantities depends greatly upon the experimental situation (beam,[2] laser induced fluorescence detection,[3] time-resolved UV absorption during[31] and after[32] irradiation, or bulk IR-photolysis yield measurements). The evaluation of bulk measurements has been discussed in some detail notably in Refs. 33–35 for various irradiation geometries (including focused beams) and in Ref. 36 for Gaussian beams. We shall use here a new data treatment for practically parallel beams with arbitrary, smooth fluence profile (including, of course, Gaussian beams). The data treatment is selected to provide reliable values of $k_I(st)$, Eq. (4).

The basis for the evaluation is the master equation for URIMIR providing time dependent level populations p_k[5,37–41]

$$\dot{\mathbf{p}} = \mathbf{K}\mathbf{p} \; . \tag{16}$$

The sum of all p_k gives F_R, the remaining reactant fraction. Summing over ground and all excited levels below the threshold energy E_T for reaction one obtains F_R^*, and summing over superexcited levels above the threshold energy E_T one obtains F_R^{**} ($F_R = F_R^* + F_R^{**}$). The general expressions for reactant concentrations and rate coefficients are[6,22]

$$F_R^{(*)} = \sum_K \phi_K^{(*)} \exp(\lambda_K t) \; , \tag{17a}$$

$$\begin{aligned} k^{(*)}(t) &= -\frac{d \ln F_R^{(*)}}{dt} \\ &= -\left[\sum_K \lambda_K \phi_K^{(*)} \exp(\lambda_K t)\right]\left[\sum_K \Phi_K^{(*)} \exp(\lambda_K t)\right]^{-1} \; . \end{aligned} \tag{17b}$$

These equations are equally valid for the unstarred quantities F_R and $k(t)$, with the characteristic populations ϕ_K and for the starred quantities F_R^* and $k^*(t)$ with the characteristic populations ϕ_K^*.[6] The λ_K are the eigenvalues of $\mathbf{K}$. The steady state rate coefficient is from Eq. (17) with $t \to \infty$

$$k(st) = k^*(st) = -\lambda_1 \; . \tag{18}$$

λ_1 is the largest eigenvalue of $\mathbf{K}$. Equations (17) and (18) are exact for irradiation with constant intensity and irreducible $\mathbf{K}$. F_R corresponds to observation at time t, F_R^* to observation at $t \to \infty$ after irradiation during a time interval t (idealized bulk photolysis measurement). If $-\lambda_1$ is approximately proportional to the radiation intensity I over the interval of interest one has furthermore with $dF = I dt$ and a constant $k_I(st)$

$$\lim_{F \to \infty}\left(-\frac{d \ln F_R^{(*)}}{dF}\right) = \frac{k(st)}{I} = k_I(st) = -\kappa_1 \; . \tag{19}$$

Equation (19) would be exact for irradiation with constant intensity I, even with an arbitrary intensity dependence of $k(st)$. In a more typical situation, where fluence is changed by changing intensity at constant pulse duration, $k_I(st)$ should be a slowly varying function of I in the intensity ranges used. In case B,[5] in particular, one has such an approximate intensity independence of $k_I(st)$ over a sufficient range of intensities.

Measuring yields close to steady state (i.e., at high yields $\geq 30\%$) as a function of uniform fluence, one would directly obtain κ_1 or $k_I(st)$ according to Eq. (19). This would be possible with the hypothetical rectangular beam profile in Fig. 1. In practice, with a smooth fluence profile, even at high overall yields P_{app} one has contributions from irradiation in the wings with low F, small yields, and far away from steady state. It is then useful to start from the complete expansion for F_R^* (in terms of fluence as independent variable)[6]

$$F_R^* = \sum_K \phi_K^* \exp(\kappa_K F) \; . \tag{20a}$$

For a useful fit to data, this expansion must be truncated after a few terms (only one or two exponentials below). One has to add then the condition

$$F_R^* = 1 \text{ for } F \leq F_m \; . \tag{20b}$$

This avoids $F_R^* > 1$ resulting from the truncated Eq. (20a). For example with one exponential, corresponding to steady state, F_m would be the intercept at the F axis of the steady-state straight line in the logarithmic reactant fluence plot (i.e., the characteristic fluence F_1^*).[6]

Another useful function representing the yield approximately also far from steady state is based on the activation equation[8] for the time dependent rate coefficient (activation time θ).

$$k(t) = k(st) \exp[-(\theta/t)^2] \; . \tag{21}$$

For F_R^* one obtains from this in terms of fluence

$$F_R^* = \exp\left\{-\int_0^F k_I(st) \exp[-(\varphi/x)^2]\right\} dx \; , \tag{22a}$$

$$F_R^* = \exp\left\{\tfrac{1}{2} k_I(st)\, \varphi\left[2\sqrt{\pi} + \sum_{n=0}^{\infty} \frac{(-1)^n}{n!\,(n-1/2)}\left(\frac{\varphi}{F}\right)^{2n-1}\right]\right\} . \tag{22b}$$

Equations (21) and (22) have been shown to give good approximate representations for all relevant product yields $1 > F_p^* > 0.001$ under typical conditions.[8] Equation (22) is a two parameter function with the activation fluence φ and the desired parameter $k_I(st)$, which is the same as in Eq. (19). Other approximate few parameter expressions have also been suggested more recently,[20,42] which we shall not use here.

With the approximate expressions in Eqs. (20) and (22) we can now obtain the fraction f of reactant decomposed, by integration or by summation over the surface elements δQ_i of the reaction cell cross section Q

$$f = \sum_i \frac{\delta Q_i}{Q} F_{p(i)}^* \; , \tag{23}$$

$$F_{p(i)}^* = 1 - g(c_i F) \; . \tag{24}$$

One can finally normalize to the nominal beam cross section Q_B (see rectangle in Fig. 1) by multiplication with Q/Q_B and obtain P_{app} in Eq. (15)

$$P_{\text{app}} = \sum_i \frac{\delta Q_i}{Q_B}[1 - g(c_i F)] \; . \tag{25}$$

F is the nominal fluence, $F_{\max}$ in Fig. 1, and $c_i F$ is the fluence F_i taken to be constant for the small surface element δQ_i. The $\delta Q_i/Q_B$ and the $c_i \leq 1$ are a set of constants to be determined once for a set of experiments from the measured fluence profile of the beam, e.g., Fig. 1. We imply that $Q_B \ll Q$ and that therefore the yield at the cell walls vanishes. The function g may be taken from either Eq. (20) or (22). The final expression using Eq. (20), e.g., would be [with the unit step function $h(x>0)=1$, $h(x<0)=0$]

$$P_{\text{app}}=\sum_i \frac{\delta Q_i}{Q_B}\left[1-\sum_{K=1}^{N}\phi_K^*\exp(\kappa_K c_i F)\right]h(c_i F-F_m) \quad . \qquad (26)$$

This is a function of $2N$ parameters (in practice $N=1$ or 2) to be fitted to the measured P_{app} from Eq. (15). Similarly one obtains a two parameter expression from the activation Eq. (22). The above discussion is straightforward. The important point is the use of theoretical functions in which $k(st)$ appears explicitly and is the *dominant* parameter when P_{app} is large. The discussion could be given as well in terms of volume elements, thus becoming applicable to focused geometries, but we think that parallel irradiation geometries are preferable. The treatment applies to any well defined and measurable fluence profile (defining the set of constants $\delta Q_i/Q_B$ and c_i), not just to Gaussian beams.

The mathematical evaluation of experimental data with Eq. (25) requires a nonlinear least squares fit. We have mainly used for this Marquardt's maximum neighborhood method,[43] which we found efficient in the present context, particularly because of the simple nature of the theoretical fit functions and their derivatives with respect to the parameters, which are required for the algorithm. However, there are many alternatives and the subject has been dealt with in a recent review.[44]

We have also derived another evaluation of $k(st)$ using the deconvolution of Ref. 36, which is valid for Gaussian beams only. This results in an expression with three parameters $J(F_S)$, F_1^*, and $k_I(st)$ (see Appendix for the derivation)

$$P_{\text{app}}(F\geqslant F_S)=J(F_S)+\int_{F_1^*}^{F}x^{-1}\{1-\exp[-k_I(st)(x-F_1^*)]\}dx \quad . \qquad (27)$$

This function is based upon the assumption that steady state applies above some value F_S of the fluence and works very well for the somewhat restricted case of Gaussian beams, if F_S is chosen properly [this is always possible by trial and error using the condition, say $F_p^*(F_S)>0.3$].

In order to illustrate the efficiency and limitations of the above equations for the evaluation of true yields and rate coefficients from apparent yield data, we show first the result of a theoretical simulation for a molecular model of CF$_3$I. Photolysis yields F_p^* as a function of fluence [Eq. (17a)] have been calculated theoretically as discussed in detail in Refs. 8 and 22. For simplicity, we considered only case B and set the bandwidth parameter $(\epsilon_1/\Delta E)\simeq 4$ (see Sec. 3.1 of Ref. 6). From F_p^* apparent yields P_{app} have been calculated for an ideal Gaussian beam profile using Eq. (25) and the exact Eq. (17) for g. One obtains the points in Fig. 3(a) ("experimental result"). These points have been fitted as discussed above. One exponential in Eq. (20a), corresponding to the assumption of steady state throughout, gives the best fit (line) shown in Fig. 3(a). Using two exponentials in Eq. (20a), or Eq. (22), or the three parameter fit of Eq. (27) gives best fits right through the exact points and are not shown in the figure. Figure 3(b) shows the functions $-\ln F_R^*=f(F)$ calculated from the various best fit expressions. The points indicate again the true values. The two parameter steady state approximation obviously deviates somewhat from the true values, giving, however, only about 30% error in $k(st)$. The three-parameter steady state expression from Eq. (27) fits well at high yields and Eq. (22) with two exponentials gives a practically perfect fit (dashed line) with only 1.5% error in $k(st)$, and a somewhat less good result is obtained from the two parameter activation equation (not shown in order to avoid crowding the figure). With a sufficient number of points we have tested the method to converge for ten exponential terms to the known correct values of the ϕ_K^* and κ_K. This is not a practical result, because experimental error for any real-life P_{app} will make such a high order fit unstable.

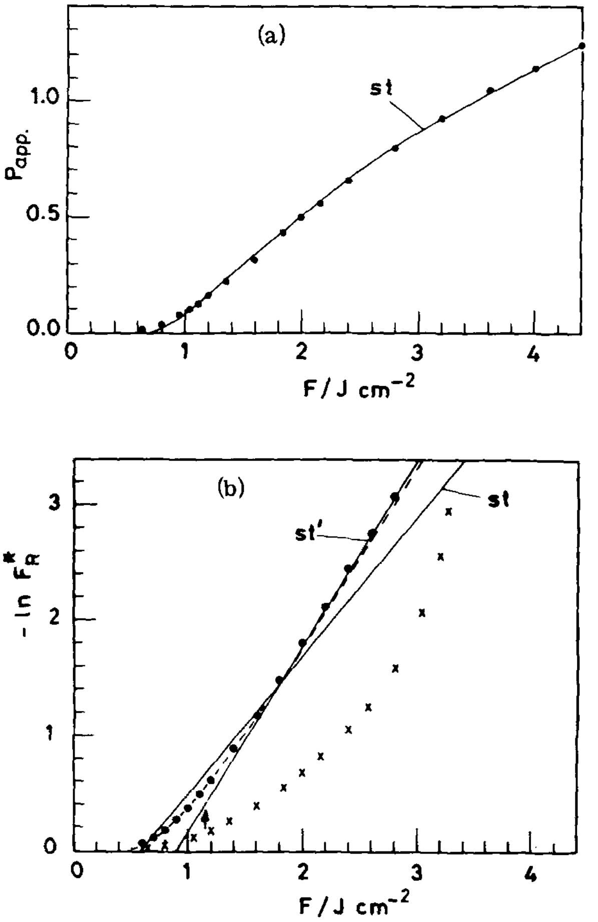

FIG. 3. (a) Apparent yield P_{app} from a model calculation for CF$_3$I photolysis and a Gaussian beam profile (see the text and Ref. 8 for details of the model). The full line is from a least squares fit using the steady state assumption [one exponential term in Eq. (20)]. (b) True values of $-\ln F_R^*$ for the model of CF$_3$I photolysis (points). The dashed line is calculated with the parameters of a two exponential term least squares fit to P_{app} of Fig. 3(a), the straight lines are from the steady state expression [st from Eq. (20), st' from Eq. (27)], and the crosses are calculated with the approximation $1-F_R^*=P_{\text{app}}$, a commonly used but poor approximation.

Additional parameters that might be considered are the intercepts on the F axis from the steady state expressions (characteristic fluence F_1^*) or the activation fluence φ in Eq. (22). For these one has in the present example $F_1^* = 0.6$ and 0.9 J cm^{-2} (steady state lines) and $\varphi = 0.72$ J cm^{-2} for the activation equation. The latter two parameter equation gives an adequate representation of yields even in the nonsteady state regime. The same is true for the fit with Eq. (20) and two exponential terms, shown by the dashed line in Fig. 3(b). For reasons that will be discussed in Sec. III D, we shall, however, attach less physical significance to the additional parameters obtained when fitting these expressions to experimental results.

B. IR photolysis of CF_3I at low pressures

Photolysis yields of CF_3I using various scavengers are shown in Fig. 4(a). The total pressure in the runs was about 150 Pa, the partial pressures of CF_3I were always less than 13 Pa. This suppressed C_2F_6 formation in all but the runs with NO at high fluences, for which appropriate corrections were applied. It is seen that the photolysis yields of all reaction mixtures agree within experimental scatter, thus supporting the interpretation as primary yields (see also Sec. II). Furthermore, results using the short pulse (open circles) agree with the ones using the long pulse (points). This indicates that under our conditions the intrinsic nonlinear intensity dependence is not very large. This may be understood in terms of the very intense, short pulses (Fig. 2) and of the moderate pressure reducing any case C effects that are expected for this reaction at moderate intensities.[22] It may be pointed out that the test is not very stringent and small nonlinearities at low fluence cannot be excluded. Larger nonlinear effects have been found in Ref. 14 (see also Ref. 53).

All results shown in Fig. 3(a) have been obtained by irradiation with the $R14$ line of the ($001 \rightarrow 02^00$) transition at 1074.65 cm^{-1}. This is close to the center of the Q branch of the parallel transition corresponding to the $\nu_1(A_1)$ CF_3 symmetric stretching fundamental at 1075.2 cm^{-1}. We have measured the frequency dependence of the yields at intermediate fluence, which shows a broad maximum near the $R14$ line (much broader than the small signal absorption cross section). This is qualitatively consistent with the finding in.[14] The rates reported below are thus close to the maximum rates, in which we are interested.

Figure 4(a) contains also two fits to these data, one approximating the real pulse shape by a Gaussian (cf. Fig. 1) and taking two exponentials in Eq. (20) (full line). This gives the true yield in Fig. 4(b) indicated by the full line labeled 2 and a steady state rate coefficient $k(st) = 1.59 \times 10^6$ $(I/\mathrm{MW\,cm^{-2}})\,\mathrm{s^{-1}}$. The second fit involves the true spatial fluence profile and the activation Eq. (22) (dashed line). There is a systematic improvement of the fit (also with the other fit functions) at high yields, which is easily understood to be due to the wings of the fluence profile. The rate coefficient is from this $k(st) = 1.56 \times 10^6$ $(I/\mathrm{MW\,cm^{-2}})\,\mathrm{s^{-1}}$. Another fit to the data is shown only in Fig. 4(b), being based on the steady state assumption (straight line), Eq. (27).

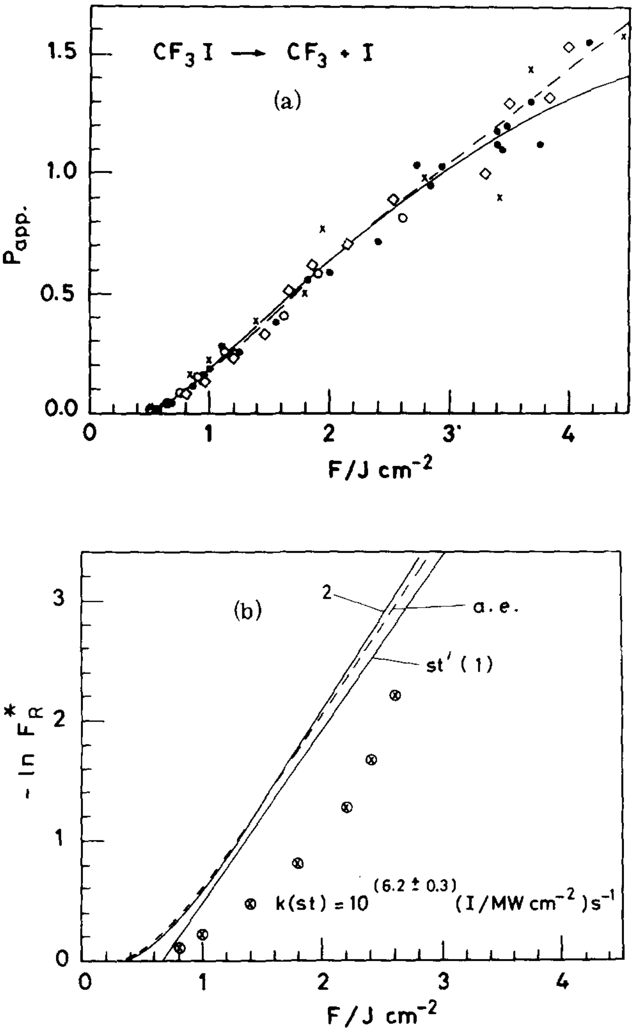

FIG. 4. (a) IR photolysis yield for irradiation of CF_3I at 1074.65 cm^{-1} with various scavenger gases and pulse conditions. ●: NO, long pulse; ○: NO, short pulse; X: ClNO long pulse; ◇: Br_2 long pulse. The full line is from a least squares fit using Eq. (20) with two exponentials, assuming a Gaussian fluence profile, and the dashed line is from the activation Eq. (22) using the measured fluence profile including the wings (see Fig. 1). (b) True $-\ln F_R^*$ functions calculated from the parameters of the experimental results using various theoretical functions: 2 is the two term exponential, Eq. (20), st' is from Eq. (27), and a.e., is from the activation Eq. (22). The points (⊗) are from the approximation $1 - F_R^* \simeq P_{app}$.

This gives a rate coefficient $k(st) = 1.45 \times 10^6$ $(I/\mathrm{MW\,cm^{-2}})\,\mathrm{s^{-1}}$ and $F_1^* = 0.7$ J cm^{-2}. The scatter of these values gives also some indication of the uncertainties, which are introduced just by the fit functions. A good value for the rate coefficient is finally

$$k(st) = 10^{(6.2\pm0.3)}\,(I/\mathrm{MW\,cm^{-2}})\,\mathrm{s^{-1}} \ .$$

The error estimate includes systematic errors due to various uncertainties. Whereas at high yield the various fits give fairly close agreement with the true yields, the approximation $F_p^* = P_{app}$: also shown in Fig. 4(b) (circles), is poor.

One may compare the yields and rates of Fig. 4(b) with previous results, where invariably the approximation $P_{app} \simeq F_p^*$ has been used, but sometimes with somewhat more favorable, flatter, although less well defined fluence profiles. Our results are higher than all previous ones. The earliest ones, still uncorrected for the recombination CF$_3$+I, gave a rate coefficient[7,11] $k(st) = 1.1 \times 10^5$ $(I/\mathrm{MW\,cm^{-2}})\,\mathrm{s^{-1}}$. In Refs. 14 and 16 primary yields were obtained with a rate coefficient of about $(4 \pm 1) \times 10^5$ $(I/\mathrm{MW\,cm^{-2}})\,\mathrm{s^{-1}}$ for the $R16$ line (the differences are largely *not* due to the difference in frequency, which gives only a small change). The best agreement is obtained with the data of Ref. 17, from which a rate coefficient of about 8×10^5 $(I/\mathrm{MW\,cm^{-2}})\,\mathrm{s^{-1}}$ has been evaluated.[8] One may also compare to an absolute *a priori* low estimate of the rate coefficient in case B with the simple theoretical model of Ref. 8, which gives 4×10^5 $(I/\mathrm{MW\,cm^{-2}})\,\mathrm{s^{-1}}$, a factor of 4 lower than the experimental one. In view of the nature as a low estimate without any adjustable parameters, this can be considered to be good consistency. If one compares the theoretical model calculation in Fig. 3, in which just one parameter has been roughly adjusted, and the experimental result of Fig. 4 one finds quite good agreement. In any case we can conclude here that our current *experimental* result for $k(st)$ can be considered to be definite and reliable. The physical significance of this result and the dependence upon experimental boundary conditions will be further discussed in Sec. III D, after consideration of collisional effects.

C. Results at high buffer gas pressures

As other results obtained in bulk situations the above experiments are not truly collisionless. On the other hand, thermal heating, or nonthermal vibrational heating by energy transfer between the laser excited reactant molecules, contributes negligibly to the reaction, which is truly photochemical under our conditions. The question arises as to the influence of the collisions with the scavenger gases. The role of collisions with buffer gases has been investigated in several papers for SF$_6$,[45,46] CF$_2$HCl,[47] CF$_2$CFCl,[48] and tetramethyldioxetane IR photolysis.[49] In the present section, we shall investigate how the evaluation of $k_I(st)$ presented above depends upon collisions with an excess of buffer gas molecules. It will be seen that to a first approximation the effect upon the *apparent* $k_I^a(st)$ from the slope of appropriate logarithmic reactant fluence plots is small, much smaller than the effect upon absolute yields and the *true* $k_I(st)$.

We shall first show with a model calculation how collisions are expected to affect the logarithmic reactant fluence plot and P_{app}. The simplest approximate procedure to take into account theoretically the effects of collisions is to add collisional terms to the master Eq. (16).[5,20,21,47–49,54,55]

With this collisional model and the radiative matrix as discussed before we have solved Eq. (16) and calculated the true yield $F_p^{(*)}$ and the apparent P_{app} for a Gaussian spatial fluence profile and pulses of constant duration as discussed in Sec. III A. The fluence is varied proportional to intensity in order to represent the typical experimental conditions. The results of the calculation for a model of CF$_3$I are shown in Fig. 5(a) for $[M]$ increasing as 1 : 10 : 100. The absolute pressures of a typical diatomic buffer gas at room temperature would be about 40 : 400 : 4000 Pa, to give an order of magnitude, not too relevant here. For the lowest pressures the effects are seen to be minor, whereas at high pressures there is considerable quenching.

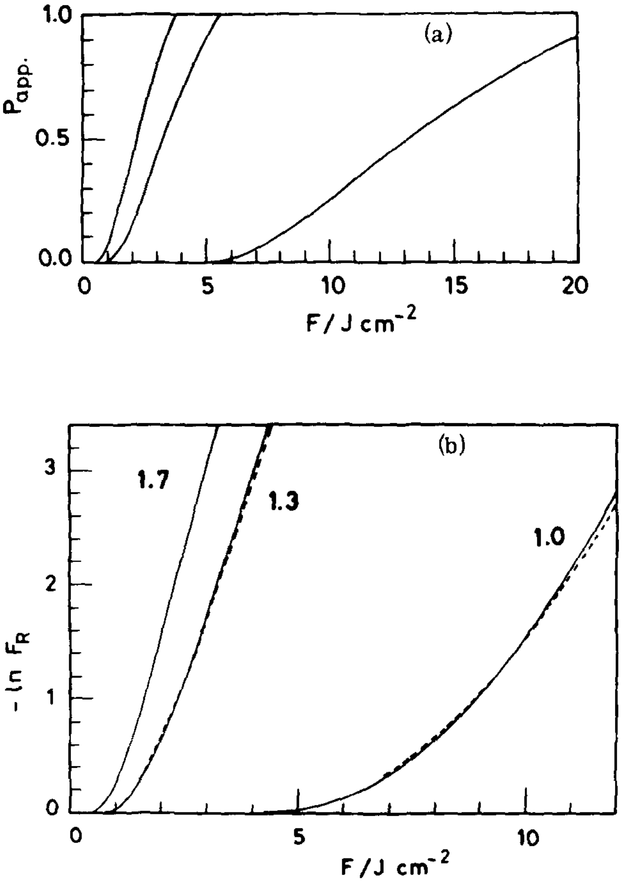

FIG. 5. (a) P_{app} calculated under collisional conditions from the model described in the text. The buffer gas pressure increases for the functions from left to right as 1 : 10 : 100. (b) True $-\ln F_R$ functions (full lines) calculated for the model as in (a) and from least squares fits to P_{app} using the activation Eq. (22) (dashed lines, coinciding with the full lines where not shown). The numbers indicate the values of $k_I^a(st)$ in cm^2 J^{-1}.

The apparent yields of Fig. 5(a) have been fitted with Eqs. (20) and (22) as discussed in Sec. III A. The parameters have now a completely different meaning and are taken to be empirical parameters approximately describing the form of the yields as a function of fluence (we use an exponent a in the notation for these parameters). It turns out that the $-\ln F_R$ functions in Fig. 5(a) calculated from the fits with the approximate equations (notably the activation equation, dashed line) closely approximate the true values [full lines in Fig. 5(b)]. The empirical parameter $k_I^a(st)$ is rather insensitive to vast changes in pressures and yields. It first increases somewhat above the (theoretical) collision-free value of $k_I(st)$ (1.6 cm^2 J^{-1}, see Sec. III A) and then decreases slowly with increasing pressure. It should be stressed that the parameter $k_I^a(st)$ in the collisional case is not at all equal to the actual steady state rate

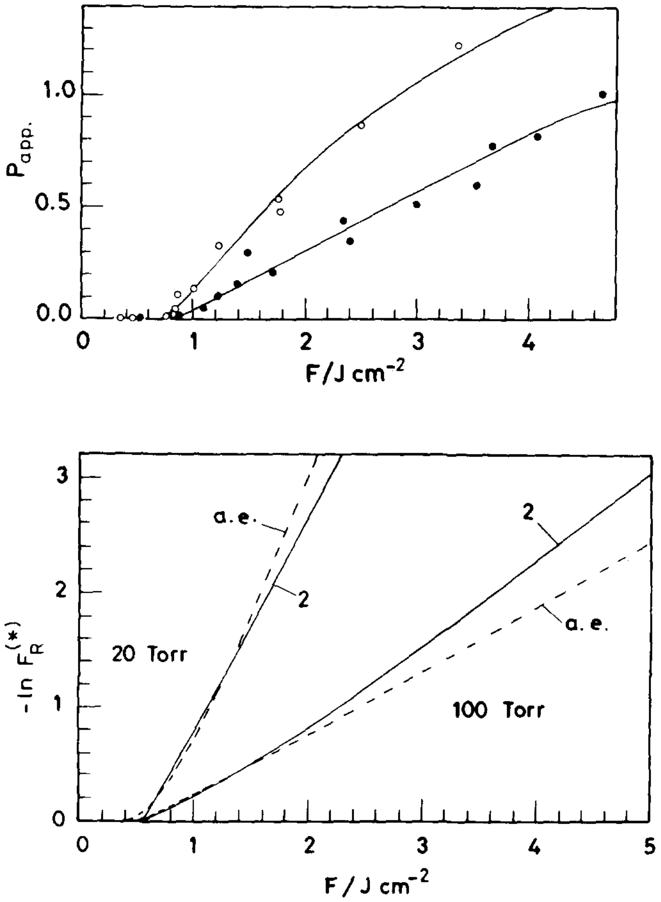

FIG. 6. (a) Experimental results for the IR photolysis of CF_3I with buffer gas pressures of $p_{NO} = 260$ Pa (○) and $p_{NO} = 1300$ Pa (●). (b) True $-\ln F_R^{(*)}$ functions calculated from the parameters of least squares fits to P_{app} in (a), using a two-term exponential (2) or the activation equation (a.e.).

coefficient, which could be obtained from a logarithmic reactant fluence plot by changing fluence at constant intensity (i.e., $F \propto$ pulse duration t), e.g., by using the technique of pulse shaping of Ashfold, Atkins, and Hancock.[4] In fact, at a typical intermediate intensity, giving $-\ln F_R \simeq 1.68$ for the collisionless case one has a reduction of $-\ln F_R$ by collisions to $0.92 : 0.38 : 3.3 \times 10^{-6}$ of the collisionless value for the pressures shown (we compare the unstarred quantities, because collisional quenching after irradiation is important at the higher pressures). Similarly, the true $k_I(st)$ is reduced to $0.92 : 0.39 : 2.2 \times 10^{-6}$ of the collisionless value.

The insensitivity of the constant $k_I^a(st)$ obtained from the slope of the logarithmic reactant fluence plot when changing F proportional to I under collisional conditions can be understood on two grounds. Firstly, the yields have to be evaluated in fluence and intensity ranges where the yield is large and the intensity high. Therefore, the collisional quenching competes relatively little with optical pumping, and in these intensity ranges, which are *different* for different pressures, $k_I(st)$ is not so different from the collision-free value, although at *constant* intensity the changes of $k_I(st)$ with pressure are pronounced. Secondly, when changing fluence and intensity under collisional conditions, the low fluence parts of the logarithmic reactant fluence plots will be more strongly affected than the high fluence parts. This increases the slope and counteracts any decrease of $k_I(st)$. These cancellations are, of course, only approximate. They are, however, quite general, as we have established in a series of model calculations. This useful insensitivity of $k_I^a(st)$ is also nicely borne out by experiments with high buffer gas pressures.

Figure 6(a) shows P_{app} from the IR photolysis of CF_3I with pressures $p_{NO} = 260$ Pa (open circles) and $p_{NO} = 1300$ Pa (points). For some measurements at total buffer gas pressures of 1300 Pa a 4 : 1 mixture of $N_2 : NO$ was used, which gives the same results as with NO. In all experiments one has $p_{CF_3I} \leq 13$ Pa and irradiation with the $R14$ line as discussed in Sec. III B. The full lines in Fig. 6(a) correspond to fits by a two exponential term Eq. (20). From these fits one obtains the $-\ln F_R$ functions in Fig. 6(b), whereas the activation equation fits [not shown in Fig. 6(a)] lead to the functions represented by the dashed lines. The differences give an indication of the uncertainties introduced by the fit functions. They become large only for large $-\ln F_R$, i.e., when F_p is close to unity, where the differences do not have much physical significance. At 260 Pa the values of $k_I^a(st)$ are 1.97 $cm^2 J^{-1}$ (2 exponential fit) and 2.85 $cm^2 J^{-1}$ (activation equation), that is larger than the true collisionless value (1.6 $cm^2 J^{-1}$). The fact that at 260 Pa $-\ln F_R$ (in the range > 2) is larger than the collisionless values is an artifact due to this large slope, since P_{app} is below the collisionless values. At 1300 Pa buffer gas pressure one obtains $k_I^a(st) = 0.78$ $cm^2 J^{-1}$ (2 exponential fit) and $k_I^a(st) = 0.57$ $cm^2 J^{-1}$ (activation equation). The important result in agreement with the theoretical calculations is that the apparent $k_I^a(st)$ are still quite close to the true collisionless values under severely collisional conditions with buffer gases. This finding can be helpful for the approximate determination of rate coefficients $k_I(st)$, when for some reason moderate buffer gas pressures are required. The concentration of reactant *must* remain always small, though. The small amounts of buffer gas present in the results of Sec. III B do not seriously affect the values of $k_I(st)$ as compared to the true collisionless case. In fact, in terms of a transition to the linear regime of URIMIR some buffer gas may be beneficial,[22] as we shall also discuss in the following section. Furthermore, in bulk measurements some added buffer gas helps avoiding problems due to collisional vibrational heating of reactant molecules (V–V transfer) and diffusion to the walls, thus providing better controlled experimental conditions.

D. The physical significance of the experimental rate coefficients

In an ideal situation in the linear regime of URIMIR (case B[5]) and with an irreducible rate coefficient matrix the values of $k_I(st)$ derived by the procedure discussed above from simple reaction yield measurements as a function of fluence contain information upon the absolute rates accessible also in time resolved measurements. For instance, a time resolved concentration measurement under irradiation with constant intensity[4] is predicted to provide a rate coefficient $k(st) = k(t \rightarrow \infty)$

$= k_I(st) \cdot I$. The evaluation of $k_I(st)$ thus solves the kinetic problem in IR photochemistry, which is equivalent to the measurement of the absolute reaction rate constant in ordinary chemical kinetics. Some complications arise in real-life situations, which we shall discuss briefly (see also Ref. 23).

At low intensities, in the nonlinear regime of URIMIR, the yield measurements would have to be made at constant intensity. Otherwise, for small molecules such as CF_3I at the lower fluences and intensities the experimental result strictly cannot be evaluated with the equations assuming an intensity independent $k_I(st)$. However, the evaluation stresses the results at high yields, where the linear regime is closely attained as seems certainly to be the case for CF_3I. Therefore, the $k_I(st)$ are not very sensitive to this problem. We note that absolute yields F_p^* may depend much more sensitively upon laser intensity (differences in F_R^{**}[6]) also in the linear regime of URIMIR. Thus, for the determination of $k_I(st)$ the control of fluence is sufficient (in the linear regime) and $k_I(st)$ is a transferable reaction parameter independent of a detailed control of intensity time profiles and spectral purity within the laser line, whereas the yields (both P_{app} and F_p^*) in general are not transferable.

The second complication is due to the fact that the rate coefficient matrix is really reducible for energy shells separated by more than the typical coupling bandwidths,[7] at most a few cm^{-1} at ordinary laser intensities. Many such energy shells are populated at room temperature (for an initial temperature of 0 K the rate coefficient matrix would be strictly irreducible). In practice, the rate coefficient $k_I(st)$ corresponds to an average value as noted before.[7] Such an average value is particularly simple if all energy shells have the same $k_I(st)$. This situation may sometimes prevail for large molecules. For a dense distribution of different values of $k_I(st)$, there is no great difficulty in the interpretation of the average value, which will depend upon the initial population of energy shells and therefore upon temperature.[6,52] For CF_3I, there is good indication from the experimental fluence dependence that such a dense distribution with a meaningful average $k_I(st)$ applies. Otherwise a turnover would be observed as for CF_2HCl.[23] We note that the form of Eq. (20) is able to cover cases with reducible K and turnovers, but the fit does not give any indication of an important contribution of this kind. We mention that the simple partitioning into two ensembles, one reactive with a given rate at a given intensity, one nonreactive (*q* factor of Ref. 17) does not appear to be realistic for CF_3I (see also the more complete theoretical discussions in Refs. 6 and 22).

Collisions couple the different energy shells discussed above and thus make K irreducible. We have seen that the effects of collisions on $k_I^a(st)$ are small, as expected. Thus a well-defined amount of added buffer gas can quite generally help to establish conditions that are reproducible with respect to collisional effects. Whereas absolute yields are strongly affected by collisions, the parameters $k_I^a(st)$ remain close to the true values $k_I(st)$ in the absence of collisions, assuming that the intensity is high enough to reach the linear regime with an effectively irreducible K. On the other hand, the other parameters of the fits to the yield functions (φ, ϕ_1^*, ϕ_2^*, etc.) are sensitive to collisional effects, intensity effects, and other difficult to control experimental boundary conditions and are therefore exluded from the detailed discussion here. This does not imply that these additional parameters are unimportant for the dynamics of URIMIR. However, a meaningful experimental determination will be possible only, if at least irradiation with constant intensity is achieved.[4] Since this will be practical at present only for few cases, we strongly recommend the evaluation of $k_I(st)$ as a meaningful dynamical parameter. We think that it is to be preferred over the parameters of the LNDF suggested by Barker,[20] although Barker's presentation of data appears to have considerable merits, sometimes.[21]

The rate coefficients $k_I(st)$ *are sensitive* functions of the kind of reaction and molecule considered,[8] in fact so much so that for many reactions the $k_I(st)$ and the reaction yields will be too small to be easily measured with present day techniques. The predicted absolute values of $k_I(st)$ are also strongly dependent upon certain fundamental assumptions in the theoretical treatment of URIMIR. We may mention the interesting suggestion of Carmeli and Nitzan[40] that the radiative pumping rate coefficients K_{NM} even under case B conditions *may* be much lower than the Pauli rate coefficient, derivable from the irregular phase assumption,[5] random coupling models,[39,40] or related assumptions.[41] If this were so, the measured rate coefficient for CF_3I, e.g., should be much lower than the theoretical estimate based on the Pauli rate coefficient. This appears *not* to be the case (see Sec. III B). However, the theoretical estimate depends upon poorly known molecular properties and therefore this comparison does not provide a very stringent test, yet.

IV. CONCLUSION

It is thus possible to derive a kinetic quantity, the absolute steady state rate coefficient $k(st)$, from measurements of bulk yields in IR photochemistry. The same quantity could be measured by time resolved concentration measurements under irradiation with constant intensity. If such an experiment is carried out for CF_3I photolysis, from the present experimental results we predict that

$$k(st) = 10^{(8.2\pm0.3)}\ \mathrm{s}^{-1} \ ,$$

at an intensity of 100 MW cm^{-2} and as $t \to \infty$ (in practice this value of *k* would be approached to better than a factor of two before 30% of the molecules have reacted). Although such results are still necessarily crude, as indicated by the large error limits, they are expected to be reliable, and transferable from one laboratory to another, which is not generally true for yield measurements. In the evaluation one must take care to produce well defined overall fluence and smooth spatial fluence profiles and take these into account by appropriate methods discussed in some detail in the present paper. On the other hand, the exact intensity time profile need not be controlled nor is there an absolute need to eliminate collisions with buffer gas molecules, which, on the contrary, may even be beneficial. The basic assumption is that at high yields the linear regime of URIMIR (i.e., $k(st) \propto I$, approximately) is attained. This will be possible for many molecules at moderate laser intensities. It then becomes possible to study systematically the dependence of an important kinetic quantity upon molecular properties of the reactant molecules using simple, quantitatively reliable experimental techniques. If such data become available more abundantly, they will help to answer current questions concerning the dynamics of IR photochemistry.

ACKNOWLEDGMENTS

The authors are deeply indebted to J. Troe, whose generous support has made this work possible. Help from H. Hippler, S. Hoff, and W. Knorr and many stimulating discussions with Hubert van den Bergh are gratefully acknowledged. This work was supported by the Deutsche Forschungsgemeinschaft (Sonderforschungsbereich 93, Photochemie mit Lasern) and by the Fonds der chemischen Industrie. Computing time and some software was provided by the GWD Göttingen.

APPENDIX: DERIVATION OF EQ. (27) FOR GAUSSIAN BEAMS

We write the exact yield as a steady state contribution and a correction function $A(F)$

$$-\ln F_R = k_I(st)\,(F - F_1^*) + A(F)\ , \quad \text{for } F > F_1^*\ , \tag{A1a}$$

$$-\ln F_R = 0 + A(F)\ , \quad \text{for } F < F_1^*\ . \tag{A1b}$$

We assume that above a certain value F_S of the fluence steady state applies exactly, hence

$$A(F) = 0\ , \quad \text{for } F \geqslant F_S\ , \tag{A2a}$$

$$A(F) \geqslant 0\ , \quad \text{for } F \leqslant F_S\ . \tag{A2b}$$

Introduce the function $B(F)$:

$$B(F) = \exp[-A(F)] - 1\ , \tag{A3a}$$

$$B(F) = 0\ , \quad \text{for } F \geqslant F_S\ , \tag{A3b}$$

$$-1 \leqslant B(F) \leqslant 0\ , \quad \text{for } F \leqslant F_S\ . \tag{A3c}$$

Therefore, one has for the product yields $F_p = 1 - F_R$

$$F_p = 1 - [1 + B(F)]\exp[-k_I(st)\,(F - F_1^*)]\ , \quad \text{for } F > F_1^*\ , \tag{A4a}$$

$$F_p = B(F)\ , \quad \text{for } F < F_1^*\ . \tag{A4b}$$

The following relationship between the apparent yield P_{app} and the true yield F_p has been derived in Ref. 36 for Gaussian beams (assuming implicitly that the yield close to the cell walls vanishes)

$$F_p = F\,\frac{dP_{\text{app}}}{dF}\ . \tag{A5}$$

Therefore, one has with Eq. (A4a) for $F > F_1^*$:

$$\frac{dP_{\text{app}}}{dF} = \frac{1}{F}\{1 - [1 + B(F)]\exp[-k_I(st)\,(F - F_1^*)]\}\ . \tag{A6}$$

Integration from 0 to $F > F_S$ yields

$$P_{\text{app}} = \int_0^{F_S} X^{-1}B(X)\exp[-k_I(st)\,(X - F_1^*)]\,dX + \int_{F_1^*}^{F} X^{-1}\{1 - \exp[-k_I(st)\,(X - F_1^*)]\,dX\ . \tag{27}$$

The first integral is the parameter $J(F_S) \neq f(F)$, and the other parameters are $k_I(st)$ and F_1^* as in Eq. (27). A similar derivation can be given using starred quantities F_R^*, F_P^*, etc., everywhere.

[1] N. R. Isenor and M. C. Richardson, Appl. Phys. Lett. **18**, 225 (1971); N. R. Isenor, V. Merchant, R. S. Hallsworth, and M. C. Richardson, Can. J. Phys. **51**, 1281 (1973).

[2] P. A. Schulz, A. S. Sudbo, D. J. Krajnovitch, H. S. Kwok, Y. R. Shen, and Y. T. Lee, Annu. Rev. Phys. Chem. **30**, 379 (1979).

[3] M. N. R. Ashfold and G. Hancock, in *Gas Kinetics and Energy Transfer*, edited by R. Donovan and P. G. Ashmore (The Chemical Society, London, 1981), Vol. 4.

[4] M. N. R. Ashfold, C. G. Atkins, and G. Hancock, Chem. Phys. Lett. **80**, 1 (1981).

[5] M. Quack, J. Chem. Phys. **69**, 1282 (1978); Adv. Chem. Phys. (to be published).

[6] M. Quack, Ber. Bunsenges. Phys. Chem. **83**, 757 (1979).

[7] M. Quack, J. Chem. Phys. **70**, 1069 (1979).

[8] M. Quack, Ber. Bunsenges. Phys. Chem. **83**, 1287 (1979).

[9] M. Quack and G. Seyfang (in preparation); Chem. Phys. Lett. (in press).

[10] A. B. Petersen, J. Tiee, and C. Wittig, Opt. Commun. **17**, 259 (1976).

[11] (a) S. Bittenson and P. L. Houston, J. Chem. Phys. **67**, 4819 (1977); (b) C. N. Plum and P. L. Houston, Appl. Phys. **24**, 143 (1981).

[12] M. Quack, Ber. Bunsenges. Phys. Chem. **82**, 1252 (1978).

[13] A. S. Sudbo, P. A. Schulz, E. R. Grant, Y. R. Shen, and Y. T. Lee, J. Chem. Phys. **70**, 912 (1979).

[14] M. Rossi, J. R. Barker, and D. M. Golden, Chem. Phys. Lett. **65**, 523 (1979).

[15] R. Naaman, M. J. Rossi, J. R. Barker, D. M. Golden, and R. N. Zare (to be published).

[16] D. M. Golden, M. J. Rossi, A. C. Baldwin, and J. R. Barker, Acc. Chem. Res. **14**, 56 (1981).

[17] (a) V. N. Bagratashvili, V. S. Doljikov, V. S. Letokhov, and E. A. Ryabov, in *Laser Induced Processes in Molecules*, edited by K. L. Kompa and S. D. Smith (Springer, Berlin, 1979) p. 179; (b) V. N. Bagratashvili, V. S. Doljikov, V. S. Letokhov, A. A. Makarov, E. A. Ryabov, and V. V. Tyakht, Sov. Phys. JETP **50**, 1075 (1979); (c) Y. A. Kudriavtsev and V. S. Letokhov, Chem. Phys. **50**, 353 (1980).

[18] W. Fuß and W. E. Schmid, Ber. Bunsenges. Phys. Chem. **83**, 1148 (1979).

[19] E. N. Okafo and W. Whittle, Int. J. Chem. Kinet. **7**, 273 (1975).

[20] J. R. Barker, J. Chem. Phys. **72**, 3686 (1980).

[21] A. C. Baldwin and J. R. Barker, J. Chem. Phys. **74**, 3813, 3823 (1981).

[22] M. Quack, Ber. Bunsenges. Phys. Chem. **85**, 318 (1981).

[23] M. Quack, P. Humbert, and H. van den Bergh, J. Chem. Phys. **73**, 247 (1980).

[24] A. E. Siegman, *An Introduction to Lasers and Masers* (McGraw-Hill, New York, 1971); K. Smith and R. M. Thomson, *Computer Modeling of Gas Lasers* (Plenum, New York, 1978).

[25] A. E. Siegman, IEEE J. Quantum Electron. **QE3**, 156 (1967); W. F. Krupke and W. R. Sooy, IEEE J. Quantum Electron. **QE5**, 575 (1969).

[26] J. L. Lyman, J. W. Hudson, and S. M. Freund, Opt. Commun. **21**, 112 (1977).

[27] D. S. King and J. C. Stephenson, Chem. Phys. Lett. **66**, 33 (1979).

[28] H. Van den Bergh and J. Troe, J. Chem. Phys. **64**, 736 (1976): (1976); H. Hippler, K. Luther, H. Teitelbaum, and J. Troe, Int. J. Chem. Kinet. **9**, 917 (1977).

[29] M. J. Rossi, J. R. Barker, and D. M. Golden, J. Chem. Phys. **71**, 3722 (1979).

[30] M. Quack and J. Troe, in *Gas Kinetics and Energy Transfer*, edited by P. G. Ashmore and R. J. Donovan (The Chemical Society, London, 1977), Vol. 2.

[31] R. Duperrex and H. van den Bergh, J. Chem. Phys. **71**, 3613 (1979).

[32] C. Kleinermanns and H. Gg. Wagner, Z. Phys. Chem. **118**, 1 (1979); C. Kleinermanns, Bericht 12, MPI fur Strömungsforschung, Göttingen, 1978.

[33] J. L. Lyman, S. D. Rockwood, and S. M. Freund, J. Chem. Phys. **67**, 4545 (1977).

[34] C. D. Cantrell, S. M. Freund, and J. L. Lyman, in *Laser Handbook*, edited by E. L. Stitch (North Holland, Amsterdam, 1979), Vol. 3B.

[35] J. L. Lyman, G. P. Quigley, and O. P. Judd, in *Multiple Photon Excitation and Dissociation of Polyatomic Molecules*, edited by C. Cantrell (Springer, Berlin, 1981).

[36] P. Kolodner, H. S. Kwok, J. G. Black, and E. Yablonovitch, Opt. Lett. **4**, 38 (1979).

[37] J. L. Lyman, J. Chem. Phys. **67**, 1868 (1977).

[38] E. R. Grant, P. A. Schulz, A. S. Sudbo, Y. R. Shen, and Y. T. Lee, Phys. Rev. Lett. **40**, 115 (1978).

[39] I. Schek and J. Jortner, J. Chem. Phys. **70**, 3016 (1979).

[40] B. Carmeli and A. Nitzan, J. Chem. Phys. **72**, 2054, 2070 (1980).

[41] S. Mukamel, J. Chem. Phys. **71**, 2012 (1979).

[42] J. Troe, J. Chem. Phys. **73**, 3205 (1980).

[43] D. W. Marquardt, J. Soc. Ind. Appl. Math. **11**, 431 (1963).

[44] K. L. Hiebert, ACM Trans. Math. Software **7**, 1 (1981).

[45] P. Bado and H. van den Bergh, J. Chem. Phys. **68**, 4188 (1978); R. Duperrex and H. van den Bergh, Chem. Phys. **40**, 275 (1979).

[46] C. R. Quick and C. Wittig, J. Chem. Phys. **69**, 4201 (1978).

[47] R. Duperrex and H. van den Bergh, J. Chem. Phys. **71**, 3613 (1979); A. C. Baldwin and H. van den Bergh, J. Chem. Phys. **74**, 1012 (1981).

[48] J. Stone, E. Thiele and M. F. Goodman, J. Chem. Phys. **73**, 2259 (1980).

[49] G. Yahav, Y. Haas, B. Carmeli, and A. Nitzan, J. Chem. Phys. **72**, 3410 (1980); B. Carmeli and A. Nitzan (to be published).

[50] D. C. Tardy and B. S. Rabinovitch, J. Chem. Phys. **48**, 1282 (1968).

[51] J. Troe, Ber. Bunsenges. Phys. Chem. **77**, 665 (1973); J. Chem. Phys. **66**, 4745, 4758 (1977).

[52] R. Duperrex and H. van den Bergh, J. Chem. Phys. **70**, 5672 (1979).

[53] M. J. Rossi, J. R. Barker, and D. M. Golden, J. Chem. Phys. **76**, 406 (1982).

[54] W. D. Lawrance, A. E. W. Knight, R. G. Gilbert, and K. D. King, Chem. Phys. **56**, 343 (1981).

[55] M. Quack, Chimia (to be published).